Journal of Physics: Conference Series **235** (2010) 012002 doi:10.1088/1742-6596/235/1/012002

Theoretical studies of autoionization dynamics of high Rydberg states

Yi-Hsieh Wang[1,2], H Mineo[1], S D Chao[1], Y Teranishi[3], S H Lin[2,3,4], H L Selzle[5], H J Neusser[5] and E W Schlag[5]

[1] Institute of Applied Mechanics and Center for Quantum Science and Engineering (CQSE), National Taiwan University, Taipei 106, Taiwan, ROC

[2] Research Center for Applied Sciences, Academia Sinica, Taipei 115, Taiwan, ROC

[3] Institute of Applied Chemistry, Institute of Molecular Science, Chiao-Tung University, Hsin-Chu, Taiwan, ROC

[4] Institute of Atomic and Molecular Sciences, Academia Sinica, Taipei 106, Taiwan, ROC

[5] Institut für Physikalische und Theoretische Chemie, Technische Universität München, Lichtenbergstr. 4, D-85748 Garching, Germany

E-mail: sdchao@iam.ntu.edu.tw

Abstract. In this paper we show how to employ the inverse Born-Oppenheimer approximation to establish a basis set to study zero kinetic energy (ZEKE) spectroscopy and the autoionization dynamics of the ZEKE Rydberg states. The calculations of vibrational and rotational autoionizations of a homonuclear diatomic molecule will be demonstrated as an example. The scaling laws for the autoionization rate constants are determined through nonlinear modeling of the calculated data.

1. Introduction

Zero-kinetic-energy (ZEKE) spectroscopy is a high resolution, rotationally resolved photoelectron spectroscopy (PES) to study the structures and dynamics of neutral and ionic molecules [1-4]. ZEKE spectroscopy has been increasingly used to determine the rovibronic energy levels of polyatomic molecular ions and to derive information on the dynamical and thermodynamical properties of molecular systems [4-9] and even the vibrational energy level structures of cations of biological molecules [10]. As in the case of conventional molecular spectroscopy, ab initio quantum chemistry calculation has become a powerful tool for the analysis of ZEKE spectra. This is especially true for the ionic species resulting from photoionization of bonding orbitals of the valence shell of stable and rigid molecules like hydrocarbons, which often exhibit a complex tunneling behavior necessitating careful studies of extended regions of the potential surfaces.

In a ZEKE experiment, a laser pulse will excite at least one electron to a high Rydberg state, which is just below the ionization threshold. After the excitation, these electrons would be detected by using a delayed ionizing field. Therefore, different from the conventional photoelectron spectroscopy (PES), which directly detects electrons in the continuum states, the electrons from the high Rydberg states in the ZEKE spectroscopy are observed [11-12]. For this reason, it is crucial to find a suitable representation of the high Rydberg state for studying the involved radiative or radiationless process. In this paper, we will present a theoretical model based on the inverse Born-Oppenheimer approximation

(IBOA) [13-16]. This model not only can provide a proper basis set for the system in high Rydberg states, but also for the dynamics of high Rydberg states, such as autoionization and collision [13, 17]. In section 2, we will present a mathematical derivation of IBOA and in section 3 we will show the numerical calculation of autoionization rate constants and the related scaling law.

2. Theory

2.1 Inverse Born-Oppenheimer approximation

Chao et al. [13-14] have developed a molecular theory of high Rydberg states using the inverse Born-Oppenheimer approximation (IBOA), which is a reversed version of the Born-Oppenheimer approximation (BOA). The basic idea is that we neglect the kinetic energy operator of the Rydberg electron in the Schrödinger equation, and obtain two separate differential equations. One is the ionic Schrödinger equation, whose Hamiltonian consists of the kinetic energy operators of core electrons and nuclei and the Coulomb potentials among all charged particles in a molecule. The other is the electronic Schrödinger equation of the Rydberg electron. With this separation, we can obtain the zeroth-order basis function for any atom or molecule in the high Rydberg state.

We now derive the basic equations. First, the Hamiltonian can be expressed as

$$\hat{H} = \hat{H}_{ion} + \hat{T}_e \tag{2.1}$$

where $\hat{H}_{ion}$ is the ionic Hamiltonian and $\hat{T}_e$ denotes the kinetic energy operator of the Rydberg electron. From Bohr's model of hydrogen atom, the electron in a high Rydberg state moves slowly and its position is far away from the core. Therefore, as a zeroth-order description, we can neglect the kinetic energy term, and solve the ionic Schrödinger equation

$$\hat{H}_{ion}\Theta_a\left(\vec{R},\vec{r}_c;\vec{r}\right) = U_a\left(\vec{r}\right)\Theta_a\left(\vec{R},\vec{r}_c;\vec{r}\right) \tag{2.2}$$

where Θ_a and U_a represent the wavefunction and ion energy of the parent ion at state a, respectively. Here $\vec{R}$ and $\vec{r}_c$ denote the nuclear coordinate and the coordinates of the core electrons, respectively, while $\vec{r}$ denotes the coordinate of the Rydberg electron. Notice that both Θ_a and U_a depends on the Rydberg electron coordinate $\vec{r}$ parametrically. Using the completeness theorem, we can expand the total wavefunction Ψ in terms of Θ_a.

$$\Psi = \sum_a \Phi_a\left(\vec{r}\right)\Theta_a\left(\vec{R},\vec{r}_c;\vec{r}\right) \tag{2.3}$$

Substituting equation (2.3) into the full Schrödinger equation, we have

$$\sum_a \hat{T}_e\left(\Phi_a\Theta_a\right) + \sum_a U_a\left(\Phi_a\Theta_a\right) = E\sum_a \Phi_a\Theta_a \tag{2.4}$$

where

$$\begin{aligned}\hat{T}_e\left(\Phi_a\Theta_a\right) &= \Theta_a\hat{T}_e\Phi_a - \frac{\hbar^2}{2m_e}\left(2\nabla_e\Theta_a\cdot\nabla_e\Phi_a + \Phi_a\nabla_e^2\Theta_a\right) \\ &\equiv \Theta_a\hat{T}_e\Phi_a + \hat{H}'_{IBO}\left(\Phi_a\Theta_a\right)\end{aligned} \tag{2.5}$$

Multiplying Θ_b^* on both sides of equation (2.4), integrating over the ionic coordinates, and neglecting the terms involving $\hat{H}'_{IBO}$, we obtain

$$(\hat{T}_e + U_b)\Phi_{bm} = E_{bm}\Phi_{bm} \tag{2.6}$$

and

$$\Psi_{bm} = \Phi_{bm}\Theta_b \tag{2.7}$$

Here *m* denotes the quantum numbers to specify the Rydberg electronic state. We shall denote the ionic wavefunction in the core electronic state *c* and rovibrational state *w* as Θ_{cw}; i.e., *b*=*cw*, and represent the corresponding Rydberg electronic wavefunction by Φ_{cwm}. From equations (2.2) and (2.6), we can see that the eigenvalue U_b of ionic Schrödinger equation serves as the potential energy of the electronic Schrödinger equation. It can also be interpreted that the Rydberg electron is moving on the potential energy surface provided by the ion core in the rovibronic state cw.

2.2 Perturbation and multipole expansion

In this section, we shall use the time independent perturbation theory to derive the zeroth-order wavefunction and higher order corrections. Consider a molecule containing n-1 electrons in the core and one electron in the high Rydberg state (denoted as the electron n). The ionic Hamiltonian can be expressed as

$$\hat{H}_{ion} = -\frac{\hbar^2}{2m_e}\sum_{i=1}^{n-1}\nabla_i^2 + \hat{T}_N + V \tag{2.8}$$

where $\hat{T}_N$ is the kinetic energy operator of the nuclei. Next, we can separate the interactions containing the electron *n* from *V*

$$\begin{aligned} V &= V_{ion} + \sum_{i=1}^{n-1}\frac{e^2}{r_{n,i}} - \sum_{\alpha}\frac{Z_\alpha e^2}{r_{n,\alpha}} \\ &\equiv V_{ion} + V' \end{aligned} \tag{2.9}$$

where *i* represents the *i*-th electron in the ion core, and α refers to α-th nucleus. V' can be approximated by the multipole expansion.

$$\begin{aligned} V' = &-\frac{e^2}{r_n} + \left[\sum_{i=1}^{n-1}\frac{e^2\left(\vec{r}_n\cdot\vec{r}_i\right)}{r_n^3} - \sum_{\alpha}\frac{Z_\alpha e^2\left(\vec{r}_n\cdot\vec{R}_\alpha\right)}{r_n^3}\right] + \left\{\sum_{i=1}^{n-1}\frac{e^2}{2}\left[\frac{3\left(\vec{r}_n\cdot\vec{r}_i\right)^2}{r_n^5} - \frac{r_i^2}{r_n^3}\right]\right. \\ &\left. -\sum_{\alpha}\frac{Z_\alpha e^2}{2}\left[\frac{3\left(\vec{r}_n\cdot\vec{R}_\alpha\right)^2}{r_n^5} - \frac{R_\alpha^2}{r_n^3}\right]\right\} + \cdots \\ \equiv &-\frac{e^2}{r_n} + V_d' + V_q' + \cdots \end{aligned} \tag{2.10}$$

where V_d' denotes the dipole interaction and V_q' the quadrupole interaction, and so on. Neglecting the higher order interactions, we obtain the zeroth-order wavefunctions of the ion core and the Rydberg electron. That is, equations (2.2) and (2.6) can be expressed as

$$\hat{H}_{ion}^0\Theta_{cw}^0\left(\vec{R},\vec{r}_c\right) = U_{cw}^0\Theta_{cw}^0\left(\vec{R},\vec{r}_c\right) \tag{2.11}$$

$$(\hat{T}_e - \frac{e^2}{r_n})\Phi_m^0(\vec{r}_n) = \varepsilon_m^0 \Phi_m^0(\vec{r}_n) \tag{2.12}$$

Here we can see that the solution of equation (2.11) is the wavefunction of a bare ion, which can be calculated with the conventional quantum chemistry methods, while the solution of equation (2.12) is the wavefunction of a hydrogen atom. Therefore, as the conventional hydrogenic wavefunction [18], the quantum numbers *nlm* can be used to describe the bound electron, while *klm* can be used to describe the free electron; i.e., *m*=*nlm* or *m*=*klm*. Letting $\vec{r}_n = \vec{r} = (r,\theta,\phi)$ in spherical coordinates, we have

$$\Phi_{nlm}^0 = R_{nl}(r)Y_{lm}(\theta,\phi) \tag{2.13}$$

$$\Phi_{klm}^0 = R_{kl}(r)Y_{lm}(\theta,\phi) \tag{2.14}$$

To solve equation (2.11), we can use Born-Oppenheimer approximation and the ionic wavefunction Θ_{cw} can be separated as the core electronic wavefunction φ_c and the nuclear wavefunction ψ_{cw}. That is,

$$\hat{H}_{ion}^0 = \hat{H}_e^0 + \hat{T}_N \tag{2.15}$$

$$\hat{H}_e^0 \varphi_c^0 = u_c^0 \varphi_c^0 \tag{2.16}$$

$$(\hat{T}_N + u_c^0)\psi_{cw}^0 = U_{cw}^0 \psi_{cw}^0 \tag{2.17}$$

and

$$\Theta_{cw}^0 = \varphi_c^0 \psi_{cw}^0 \tag{2.18}$$

where $\hat{H}_e^0$ denotes the Hamiltonian of the core electrons after subtracting the nuclear kinetic energy operator $\hat{T}_N$ from $\hat{H}_{ion}^0$. In the case of diatomic molecules, the zeroth-order nuclear wavefunction ψ_{cw}^0 can be expressed in spherical coordinates $\vec{R} = (R,\Theta,\Phi)$ as

$$\psi_{cv^+N^+M_N^+}^0 = \chi_{cv^+}(R)Y_{N^+M_N^+}(\Theta,\Phi) \tag{2.19}$$

where χ_{cv^+} denotes the vibrational wavefunction and $Y_{N^+M_N^+}$ denotes the rotational wavefunction with respect to the electronic state *c* of the ion core. Here $w = v^+N^+M_N^+$ denote the vibration and rotation quantum numbers.

For a homonuclear diatomic molecule, the first-order energy correction of the dipole interaction is zero, so we shall perform the first-order correction of the quadrupole term. It follows that

$$u_c^{(1)} = \langle \varphi_c^0 | V_q' | \varphi_c^0 \rangle \tag{2.20}$$

Performing the integration with respect to the core electronic coordinates $\vec{r}_c$, we can obtain the conventional expression by using quadrupole moment *Q* as functions of the nuclear coordinate $\vec{R}$.

$$u_c^{(1)} = -e\frac{Q_c(R)}{r^3}\left[\frac{4\pi}{5}\sum_{\bar{m}=-2}^{2} Y_{2\bar{m}}(\theta,\phi)Y_{2\bar{m}}^{*}(\Theta,\Phi)\right] \tag{2.21}$$

where the first spherical harmonics depends on the coordinate of the Rydberg electron, and the second one depends on that of the ion core.

2.3 The breakdown of IBOA and autoionization

The basic concept of autoionization can be understood by using the diagram in figure 1, which is based on the IBOA model. From equations (2.11) and (2.12), we can see that, in the high Rydberg state, the electron behaves like a hydrogenic electron, and the core like a bare ion. The interaction between them is very week, so we can form two independent systems, as shown in the zeroth-order Hamiltonian.

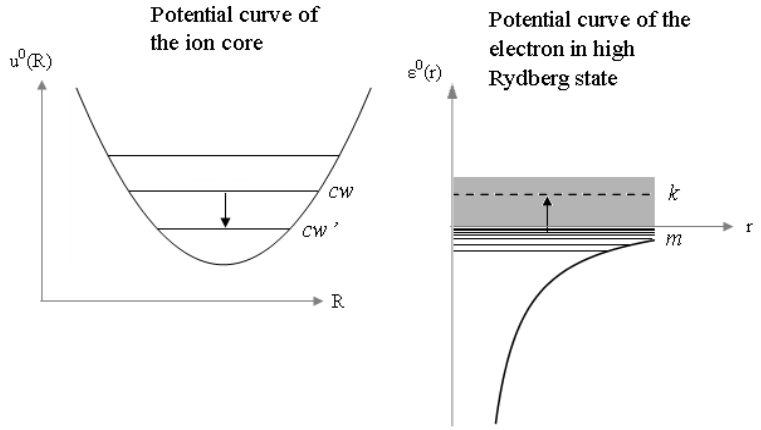

Figure 1. The diagram of vibrational autoionization based on the model of IBOA. During the autoionization $cwm \rightarrow cw'k$, the ion core would relax from a vibrationally excited state *cw* to a lower state *cw'*, while the electron in the high Rydberg state *m* would autoionize to the continuum state *k*.

As shown in the figure, the molecule was first excited to a vibrationally or rotationally excited state with one electron in the high Rydberg state. Due to the interaction within the molecule, the excited core would release its energy and transfer the energy to the Rydberg electron yielding ionization. With this understanding, we can calculate the corresponding transition rate.

Lin [19] has pointed out that within the BOA the nuclear kinetic energy operator can be used to model the radiationless processes, such as internal conversion or intersystem crossing. Likewise, here we can use the kinetic energy operator of the Rydberg electron to study the radiationless process in high Rydberg states, such as autoionization [20]. To derive the expression of the transition rate, we need to include the neglected term in equation (2.5); in other words, the radiationless transition is interpreted as the breakdown of the IBOA. Therefore, to calculate the autoionization rate, we can use the Fermi's golden rule

$$W_{(cwm\rightarrow cw'k)} = \frac{2\pi}{\hbar}\left|\left\langle \Psi_{cw'k}\left|\hat{H}'_{IBO}\right|\Psi_{cwm}\right\rangle\right|^2 \rho(E_k) \tag{2.22}$$

where $\rho(E_k)$ is the density of states for the ionized electron of energy E_k and

$$\begin{aligned}&\left\langle \Psi_{cw'k} \left| \hat{H}'_{IBO} \right| \Psi_{cwm} \right\rangle \\ &= -\frac{\hbar^2}{2m_e}\left(2\left\langle \Phi_{cw'k} \left| \left\langle \Theta_{cw'} \left| \nabla_e \Theta_{cw} \right\rangle \cdot \left| \nabla_e \Phi_{cwm} \right\rangle + \left\langle \Phi_{cw'k} \right| \left\langle \Theta_{cw'} \left| \nabla_e^2 \Theta_{cw} \right\rangle \right| \Phi_{cwm} \right\rangle \right)\end{aligned} \tag{2.23}$$

To evaluate $\nabla_e \Theta_{cw}$ and $\nabla_e^2 \Theta_{cw}$, we shall consider the first order correction of the ionic wavefunction. Using (2.19) and (2.21), we have

$$\begin{aligned}\left\langle \Theta_{cv^{+\prime}N^{+\prime}M_N^{+\prime}} \left| \nabla_e \right| \Theta_{cv^+N^+M_N^+} \right\rangle &= \frac{\left\langle \Theta^0_{cv^{+\prime}N^{+\prime}M_N^{+\prime}} \left| \nabla_e V_q' \right| \Theta^0_{cv^+N^+M_N^+} \right\rangle}{U^0_{cv^+N^+} - U^0_{cv^{+\prime}N^{+\prime}}} \\ &= -e\frac{\left\langle \chi_{cv^{+\prime}} \left| Q_c \right| \chi_{cv^+} \right\rangle}{U^0_{cv^+N^+} - U^0_{cv^{+\prime}N^{+\prime}}} \left\{ \frac{4\pi}{5} \sum_{\bar{m}=-2}^{2} \left\langle Y_{N^{+\prime}M_N^{+\prime}} \left| Y^*_{2\bar{m}} \right| Y_{N^+M_N^+} \right\rangle \nabla_e \left[\frac{Y_{2\bar{m}}(\theta,\phi)}{r^3} \right] \right\}\end{aligned} \tag{2.24}$$

$$\left\langle \Theta_{cv^{+\prime}N^{+\prime}M_N^{+\prime}} \left| \nabla_e^2 \right| \Theta_{cv^+N^+M_N^+} \right\rangle = \frac{\left\langle \Theta^0_{cv^{+\prime}N^{+\prime}M_N^{+\prime}} \left| \nabla_e^2 V_q' \right| \Theta^0_{cv^+N^+M_N^+} \right\rangle}{U^0_{cv^+N^+} - U^0_{cv^{+\prime}N^{+\prime}}} = 0 \tag{2.25}$$

Here $w' = v^{+\prime}N^{+\prime}M_N^{+\prime}$, $k = kl'm'$, $w = v^+N^+M_N^+$ and $m = nlm$, respectively. The electronic part of the quadrupole interaction V_q' is a solution of the Laplace equation, and thus the matrix element in equation (2.25) will vanish. The integration over the Rydberg electronic coordinate can be performed using the recursion relations of the hydrogenic wavefunction. For spherical harmonics, we obtain

$$\left\langle Y_{l'm'} \left| \frac{\partial Y_{2\bar{m}}}{\partial\theta} \right| \frac{\partial Y_{lm}}{\partial\theta} \right\rangle + \left\langle Y_{l'm'} \left| \frac{1}{\sin\theta}\frac{\partial Y_{2\bar{m}}}{\partial\phi} \right| \frac{1}{\sin\theta}\frac{\partial Y_{lm}}{\partial\phi} \right\rangle = D_{l',l} \left\langle Y_{l'm'} \left| Y_{2\bar{m}} \right| Y_{lm} \right\rangle \tag{2.26}$$

where $D_{l,l} = 3$, $D_{l+2,l} = -2l$, and $D_{l-2,l} = 2(l+1)$.

Therefore, we obtain the final expression of the transition matrix element as

$$\begin{aligned}&\left\langle kl'\, v^{+\prime}N^{+\prime}J\ M_J \left| \hat{H}'_{IBOA} \right| nl\ v^+N^+J\ M_J \right\rangle \\ &= -\frac{\hbar^2}{m_e}\frac{(-e)}{U^0_{cv^+N^+} - U^0_{cv^{+\prime}N^{+\prime}}} \left\langle \chi_{cv^{+\prime}} \left| Q_c(R) \right| \chi_{cv^+} \right\rangle \times \left[D_{l',l} \left\langle R_{kl'} \left| r^{-5} \right| R_{nl} \right\rangle - 3\left\langle R_{kl'} \left| r^{-4} \right| \frac{dR_{nl}}{dr} \right\rangle \right] \\ &\times g\left(l', N^{+\prime}, J', M_J'; l, N^+, J, M_J\right)\end{aligned} \tag{2.27}$$

where *nl* and *kl'* represent the quantum numbers of discrete states and that of continuum states of the ZEKE electron, respectively. The angular matrix element *g* is shown as in [21, 22]

$$g\left(l',N^{+\prime},J',M_J';l,N^+,J,M_J\right)=(-1)^{l+l'+J}\begin{Bmatrix}J & N^{+\prime} & l'\\ 2 & l & N^+\end{Bmatrix}\delta_{J',J}\delta_{M_{J'},M_J}$$
$$\times\left[(2l'+1)(2l+1)\right]^{1/2}\begin{pmatrix}l' & 2 & l\\ 0 & 0 & 0\end{pmatrix} \qquad (2.28)$$
$$\times\left[\left(2N^{+\prime}+1\right)\left(2N^{+}+1\right)\right]^{1/2}\begin{pmatrix}N^{+\prime} & 2 & N^{+}\\ 0 & 0 & 0\end{pmatrix}$$

In equation (2.27), there are three matrix elements to be calculated. The first matrix element contains the quadrupole moment of the ion core, which is a function of internuclear distance R. It is responsible for the vibrational transition. As the propensity rule of vibrational autoionization, the magnitude of the corresponding transition rate would decrease rapidly as Δv increases [23, 24]. The second one is the radial integral of the Rydberg electron, and it describes the transition from an electronic bound state to the continuum. In this section, we employed the recursion relation of associated Laguerre polynomial and performed the numerical integration to obtain the value of this matrix element. The last one involves the angular momentum for both electronic and nuclear rotation motions. Due to the symmetry of spherical harmonics, the allowed transitions should obey $\Delta l=0,\pm2$ and $\Delta N^+=0,\pm2$. In addition, the projection quantum numbers *m* and M_N^+ are summed for the coupling between the electronic orbital angular momentum *l* and the core rotational angular momentum N^+. Then, we have the total angular momentum *J* and its projection quantum number M_J. Due to the Kronecker delta, *J* and M_J are constant upon the transition. The selection rules and propensity rule of this formulation are in agreement with the previous studies of autoionization based on the multipole interaction [22] and the MQDT [25, 26].

3. Result and discussion

Here we shall calculate the autoionization rate of H_2, with respect to the transition among different rotational and vibrational states with transition $\left\{nl\ ;\ v^+N^+;\ J\ M_J\right\}\rightarrow\left\{kl'\ ;\ v^{+\prime}N^{+\prime};\ J\ M_J\right\}$.

As shown in figure 1, there is an energy restriction for autoionization, which is due to the Dirac delta function in the Fermi's golden rule. Nevertheless, in order to analyze the relation between the magnitude of transition rate and the corresponding quantum numbers, we first neglect this restriction. In the following, we will consider the transitions for different *n*, *l* and energy of the unbound state; the related transition for vibrational and rotational states is $\left(v^+=1,\ N^+=0\right)\rightarrow\left(v^{+\prime}=0,\ N^{+\prime}=2\right)$.

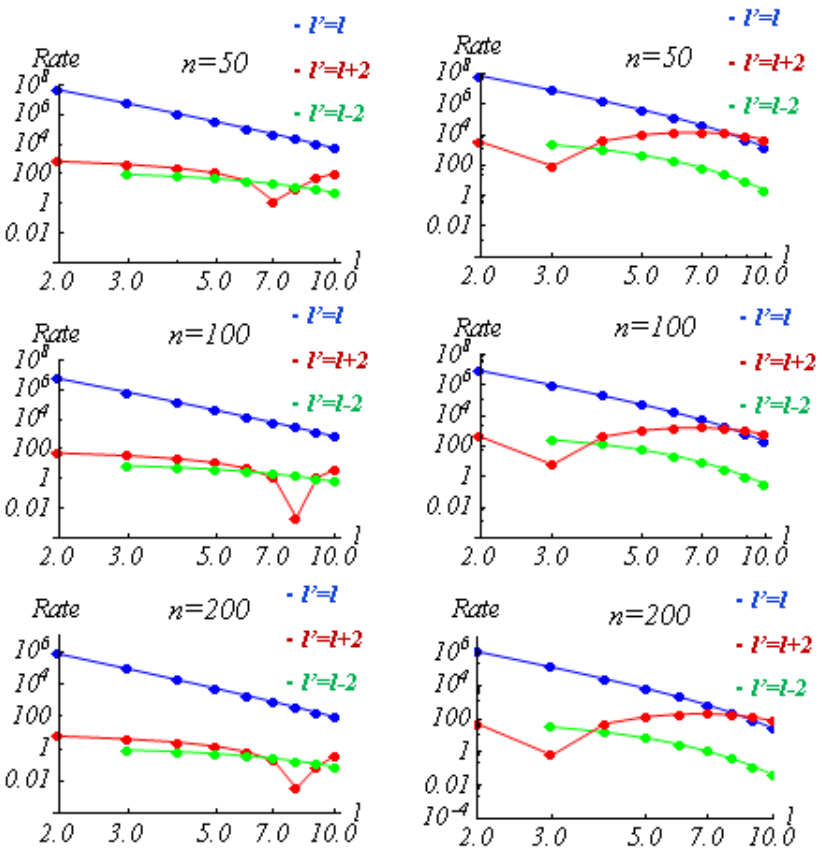

Figure 2. Comparison of the calculated autoionization rate for *l'=l*, *l'=l+2*, and *l'=l-2* in terms of the quadrupole interaction. The left panel is for the continuum-state energy of 100 cm^{-1}; the right panel is for the energy of 1000 cm^{-1}.

The numerical results calculated using equation (2.27) for H_2 are given in figure 2. If we specify the quantum numbers *n* and *k*, there are three possibilities of the final *l'* which obey the selection rule. First, in the case of *l'=l*, we can see that the rate decreases rapidly with increasing *l*. For example, the corresponding rates of *n*=100 can range from 10^3 to 10^7 s^{-1}. This behavior can be understood by the property of the hydrogenic wavefunction [18]. That is, the states at low *l* would have larger core penetration as well as stronger interaction, and thus the rate would decrease as *l* increases. Likewise, the related rate would decrease as *n* increases due to the weak interaction between the Rydberg electron and ion core. As for the *k* dependence, we found that the transition rates for low-*l* states are relatively invariant to the influence of *k*. However, those of high-*l* states have stronger energy dependence as the energy increases.

Compared with the transitions of *l'=l*, those of *l'=l+2* and *l'=l-2* are relatively slow. However, for the energy of 1000 cm^{-1}, the transitions of *l'=l+2* would compete with those of *l'=l* at larger *l* (*l*>8). Besides, from figure 2, we can see that there is no obvious tendency for these two cases. For *l'=l-2*, the rate would decrease with increasing *l* quite slowly. On the other hand, for *l'=l+2*, we can find a dip for a specific *l* in each plot. For both cases, the magnitudes of the autoionization rates are more sensitive to the energy than *l'=l*.

From figure 2, it is clear that the transition of *l'=l* shows a regular power law dependence of *l*. Using a nonlinear modeling, we obtain the scaling law for the autoionization rate as

$$rate = 3.648 \times 10^{14} n^{-3} l^{-5.3} \ s^{-1} \tag{3.1}$$

The n^3 law is consistent with that obtained from the asymptotic wavefunction of high Rydberg state. The comparison between the calculated data and the fitting curves is shown in figure 3.

In figure 3, we can see the numerical results agree well with the estimation of the scaling law for the low energy case. In equation (3.1), the scaling law is independent of the energy of the continuum state, but it still works well for the low-l transitions when the energy is relatively high. For instance, it can effectively predict the rate up to l=5 for the energy of 1000 cm^{-1}. On the other hand, for the transitions $l' = l \pm 2$, we cannot derive a scaling law of the transition rate due to the irregular dependence on l. Nevertheless, for most cases, $l'=l$ is the most probable transition, so we can neglect the contribution of $l' = l \pm 2$ transitions. In this sense, this scaling law is quite useful to gain an approximate magnitude of the autoionization rate.

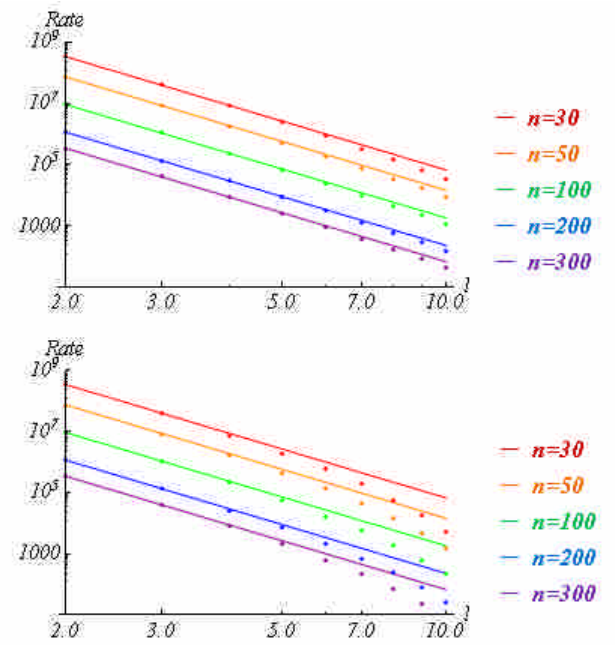

Figure 3. Comparison of the autoionization rate for Rydberg state (n,l) based on the quadrupole interaction. The upper panel is for the continuum-state energy of 100 cm^{-1}; the lower panel is for the energy of 1000 cm^{-1}. The calculated rate based on the breakdown of the IBOA is marked by point for each n, l; the lines represent the rates obtained from the scaling law.

Acknowledgements
This work is partly supported by the NSC of ROC and CQSE of NTU 97R0066-66.

References
[1] Müller-Dethlefs K, Sander M and Schlag E W 1984 *Chem. Phys. Lett.* **112** 291
[2] Schlag E W 1998 *ZEKE Spectroscopy* (Cambridge: Cambridge University Press)
[3] Cockett M C R 2005 *Chem. Soc. Rev.* **34** 935
[4] Willitsch S, Wuest A and Merkt F 2004 *Chimia* **58** 281
[5] Müller-Dethlefs K and Schlag E W 1991 *Ann. Rev. Phys. Chem.* **42** 109

[6] Merkt F 1997 *Annu. Rev. Phys. Chem.* **48** 673
[7] Ng C-Y 2002 *Annu. Rev. Phys. Chem.* **53** 101
[8] Wright T 2002 *Annu. Rep. Prog. Chem. Sect. C* **98** 375
[9] Neusser H J and Krause H 1994 *Chem. Rev.* **94** 1829
[10] Dessent C E H and Müller-Dethlefs K 2000 *Chem. Rev.* **100** 3999
[11] Merkt F and Softley T P 1993 *Int. Rev. Phys. Chem.* **12** 205-239
[12] Softley T P 2004 *Int. Rev. Phys. Chem.* **23** 1-78
[13] Chao S D, Hayashi M, Lin S H and Schlag E W 1998 *J. Phys. B* **32** 2007
[14] Chao S D, Hayashi M, Lin S H and Schlag E W 1998 *J. Chin. Chem. Soc.* **45** 491
[15] Even U, Ben-Nun M and Levine R D 1993 *Chem. Phys. Lett.* **210** 416
[16] Remacle F and Levine R D 1998 *Int. J. Quan. Chem.* **67** 85
[17] Chao S D 1999 *Thesis* (Taipei: National Taiwan University)
[18] Bethe H A and Salpeter E E 1957 *Quantum Mechanics of One- and Two- Electron Atom* (New York: Academic Press Inc.)
[19] Lin S H 1966 *J. Chem. Phys.* **44** 3759
[20] Chao S D, Selzle H L, Neusser H J, Schlag E W, Yao L and Lin S H 2007 *Z. Phys. Chem.* **221** 633-646
[21] Bixon M and Jortner J 1996 *Mol. Phys.* **89** 373-401
[22] Eyler E E and Pipkin F M 1983 *Phys. Rev.* A **27** 2462
[23] Bates D R and Poots G 1953 *Proc. Phys. Soc. (London)* **A66** 784
[24] Berry R S 1966 *J. Chem. Phys.* **45** 1128
[25] Herzberg G and Jungen Ch 1972 *J. Mol. Spectrosc.* **41** 425
[26] Raoult M and Jungen Ch 1981 *J. Chem. Phys.* **74** 3388